Monthly Notices of the Royal Astronomical Society

MNRAS **434,** 387–397 (2013)
Advance Access publication 2013 July 5

doi:10.1093/mnras/stt1027

The supermassive black hole mass–Sérsic index relations for bulges and elliptical galaxies

G. Savorgnan,[1]⋆ A. W. Graham,[1] A. Marconi,[2] E. Sani,[3] L. K. Hunt,[3] M. Vika[4] and S. P. Driver[5,6]

[1]*Centre for Astrophysics and Supercomputing, Swinburne University of Technology, Hawthorn, Victoria 3122, Australia*
[2]*Dipartimento di Fisica e Astronomia, Università di Firenze, via G. Sansone 1, I-50019 Sesto Fiorentino, Firenze, Italy*
[3]*INAF - Osservatorio Astrofisico di Arcetri, Largo E. Fermi 5, I-50125 Firenze, Italy*
[4]*Carnegie Mellon University in Qatar, Education City, PO Box 24866, Doha, Qatar*
[5]*ICRAR - The University of Western Australia, 35 Stirling Highway, Crawley, WA 6009, Australia*
[6]*SUPA - School of Physics and Astronomy, University of St Andrews, North Haugh, St Andrews KY16 9SS, UK*

Accepted 2013 June 6. Received 2013 April 22

ABSTRACT

Scaling relations between supermassive black hole mass, $M_{\rm BH}$, and host galaxy properties are a powerful instrument for studying their co-evolution. A complete picture involving *all* of the black hole scaling relations, in which each relation is consistent with the others, is necessary to fully understand the black hole–galaxy connection. The relation between $M_{\rm BH}$ and the central light concentration of the surrounding bulge, quantified by the Sérsic index n, may be one of the simplest and strongest such relations, requiring only uncalibrated galaxy images. We have conducted a census of literature Sérsic index measurements for a sample of 54 local galaxies with directly measured $M_{\rm BH}$ values. We find a clear $M_{\rm BH}-n$ relation, despite an appreciable level of scatter due to the heterogeneity of the data. Given the current $M_{\rm BH}-L_{\rm sph}$ and the $L_{\rm sph}-n$ relations, we have additionally derived the *expected* $M_{\rm BH}-n$ relations, which are marginally consistent at the 2σ level with the *observed* relations. Elliptical galaxies and the bulges of disc galaxies are each expected to follow two distinct *bent* $M_{\rm BH}-n$ relations due to the Sérsic/core-Sérsic divide. For the same central light concentration, we predict that $M_{\rm BH}$ in the Sérsic bulges of disc galaxies are an order magnitude higher than in Sérsic elliptical galaxies if they follow the same $M_{\rm BH}-L_{\rm sph}$ relation.

Key words: black hole physics – galaxies: bulges – galaxies: fundamental parameters – galaxies: structure.

1 INTRODUCTION

Observations over the past decade have suggested a strong connection between supermassive black holes (SMBHs) and their host galaxies, or rather spheroids, in spite of the huge difference between their respective sizes. While it is clear that the stories of these two objects – the black hole and the galaxy – are tightly interwoven, the origin and nature of their link are still a subject of debate. The scaling relations between the SMBH mass, $M_{\rm BH}$, and the host spheroid properties make the study of black hole growth an indispensable ingredient to understand the more general framework of galaxy formation and evolution. Beyond the well-known relation with the velocity dispersion σ (Ferrarese & Merritt 2000; Gebhardt et al. 2000; Graham et al. 2011), the masses of SMBHs have been shown to correlate with a wide series of properties belonging to the spheroidal component of the host galaxy, such as the spheroid luminosity (Kormendy & Richstone 1995; McLure & Dunlop 2002; Marconi & Hunt 2003; Graham & Scott 2013) and stellar mass (Laor 2001; Scott, Graham & Schombert 2013), the spheroid dynamical mass (Magorrian et al. 1998; Marconi & Hunt 2003; Häring & Rix 2004; Scott et al. 2013) and the central stellar concentration of the spheroid (Graham et al. 2001). The connection between bulge mass and disc galaxy morphological type means that the pitch angle of a disc galaxy's spiral arms is also related to the black hole mass (e.g. Berrier et al. 2013; Davis et al. 2013, and references therein). The old $M_{\rm BH} \propto \sigma^4$ and $M_{\rm BH} \propto L^{1.4}$ relations were actually inconsistent with each other (e.g. Lauer et al. 2007), and inconsistent with the curved $M_{\rm BH}-n$ relation (Graham & Driver 2007b) given the existence of a linear $L-n$ relation (see Section 4). The first of these inconsistencies was addressed in Graham (2012; see also section 6 of Graham 2008), and we tackle the second here. The astrophysical interest in all of these empirical relations resides partly in the fact that they must *all* be taken into account by any complete theory

⋆ E-mail: gsavorgn@astro.swin.edu.au

or model describing the co-evolution of galaxies and SMBHs, and also in their employment to predict the masses of SMBHs in other galaxies.

A decade ago Graham et al. (2001) presented evidence for a strong correlation between the stellar light concentration $C_{r_e}(1/3)$ of spheroids and their SMBH mass, showing that more centrally concentrated spheroids have more massive black holes. Graham & Driver (2007b) re-investigated the same relation, directly using the Sérsic (1963, 1968) index n as a measure of the radial concentration of the stars. In addition to a log-linear relation, Graham & Driver (2007b) fit a log-quadratic regression, finding that the $M_{\rm BH}-n$ relation changed slopes at the low- and high-mass end, and had a level of scatter equivalent to the $M_{\rm BH}-\sigma$ relation at that time ($\sim$0.3 dex). The advantages of using the $M_{\rm BH}-n$ relation to predict the mass of SMBHs are several: as noted by Graham & Driver (2007b), the measurement of n requires only images (even photometrically uncalibrated); it is not heavily affected by possible kinematic substructure at the centre of a galaxy, nor by rotational velocity or the vertical velocity dispersion of an underlying disc, nor by aperture corrections; it is cheap to acquire in terms of telescope time; and it does not depend on galaxy distances.

Pastrav et al. (2013) have recently pointed out that the recent deep, wide-field photometric surveys of galaxies – e.g. the Sloan Digital Sky Survey (SDSS, York et al. 2000) and the Galaxy And Mass Assembly (GAMA, Driver et al. 2011) – are providing us with large statistically useful samples of galaxies whose major morphological components can be resolved out to $z \simeq 0.1$. Furthermore, automatic image analysis routines, such as GIM2D (Simard et al. 2002), GALFIT (Peng et al. 2002, 2010), BUDDA (Gadotti 2008) and GALPHAT (Yoon, Weinberg & Katz, in preparation), can be used to model the surface brightness distribution of the stellar components of these galaxies (e.g. Allen et al. 2006; Simard et al. 2011; Kelvin et al. 2012). A bulge/disc decomposition, along with adequate corrections to account for dust and inclination effects as provided by Pastrav et al. (2013), can provide the Sérsic index of the spheroid component of both elliptical and disc galaxies. This can then be used to predict black hole masses in large samples of galaxies to derive the local black hole mass function (e.g. Graham et al. 2007) and space density (Graham & Driver 2007a, and references therein), if a well calibrated $M_{\rm BH}-n$ relation exists. However, in the past two years Sani et al. (2011), Vika et al. (2012) and Beifiori et al. (2012) have failed to recover a strong $M_{\rm BH}-n$ relation.

Due to the existence of the luminosity–n relation (e.g. Young & Currie 1994; Jerjen, Binggeli & Freeman 2000; Graham 2013, and references therein) and the $M_{\rm BH}$–luminosity relation (e.g. Magorrian et al. 1998), an $M_{\rm BH}-n$ relation must exist.[1] It is important to investigate why the $M_{\rm BH}-n$ relation may not have been recovered in the above studies. It is also important to know how it fits in with, and is consistent with, the other scaling relations. Not only does a proper and complete understanding of the SMBH–galaxy connection require this, but the central concentration of stars, reflecting the inner gradient of the gravitational potential, should be intimately related to the black hole mass. A well-determined $M_{\rm BH}-n$ relation may also provide an easy and accurate means to predict black hole masses in other galaxies. Eventually, semi-analytic models of galaxy formation and simulations should include in their recipes *all* of the black hole mass scaling relations.

In this work, we present a census of literature Sérsic index measurements for local galaxies with directly measured SMBH mass. We re-investigate and recover the $M_{\rm BH}-n$ relation using the combined data from four past independent works. In Section 2, we describe our galaxy sample and in Section 3, we present the $M_{\rm BH}-n$ scaling relation which is then discussed and compared with predictions in Section 4. Finally, we summarize our analysis in Section 5.

[1] It is not yet established which are the primary or secondary relations.

2 DATA

2.1 SMBH masses

Our SMBH galaxy sample comes from Graham & Scott (2013), who have built a catalogue of 80 galaxies with SMBH masses obtained from direct maser, stellar or gas kinematic measurements. Black hole masses for our final sample are listed in Table 1, along with their total galaxy B-band absolute magnitudes, $M_{B_{\rm T}}$, taken from the *Third Reference Catalogue of Bright Galaxies* (de Vaucouleurs et al. 1991, hereafter RC3) and also their morphological classification. The final sample consists of those galaxies for which Sérsic indices have been reported by at least one of the four studies mentioned below.

2.2 Collecting Sérsic indices

The radial light distribution of spheroidal systems (such as elliptical galaxies or the bulges of lenticular and spiral galaxies) is well described by the Sérsic (1963, 1968) $R^{1/n}$ model that parametrizes the intensity I as a function of the projected galactic radius R such that

$$I(R) = I_{\rm e} \exp\left\{-b_{\rm n}\left[\left(\frac{R}{R_{\rm e}}\right)^{1/n} - 1\right]\right\}$$

(Caon, Capaccioli & D'Onofrio 1993; Andredakis et al. 1995; Graham & Driver 2005, and references therein). The quantity $I_{\rm e}$ is the intensity at the effective radius $R_{\rm e}$ that encloses half of the total light from the model, and $b_{\rm n}$ is a constant defined in terms of the Sérsic index n, which is the parameter that measures the curvature of the radial light profile.

We obtained Sérsic index measurements for our SMBH sample from the following four independent works.

(i) Graham & Driver (2007b, hereafter GD07) fit the radial light profiles from a sample of 27 elliptical and disc galaxies with SMBH masses derived from resolved dynamical studies. The light profiles they used were predominantly from Graham et al. (2001), who searched the various public archives for high-quality R-band images and fit ellipses to the isophotes with the IRAF task `ellipse`, allowing the position angle and ellipticity to vary with radius.[2] The resulting light profiles were then fit by GD07 with a seeing-convolved Sérsic $R^{1/n}$ model for elliptical galaxies, and with a combined (seeing-convolved) exponential disc and $R^{1/n}$ bulge for the disc galaxies, using the subroutine UNCMND from Kahaner et al. (1989). The inner couple of arcseconds of the profiles was in some instances excluded from the fit due to the potential presence of partially depleted cores or active galactic nuclei (AGNs), that would produce a biasing central deficit or excess of light relative to the inward extrapolation of their outer Sérsic profile.

(ii) Vika et al. (2012, hereafter V12) investigated the $M_{\rm BH}-n$ and the $M_{\rm BH}-L$ relations. They performed two-dimensional (2D) profiling with GALFIT3 on near-IR images [from the UKIRT Infrared

[2] A discussion of the original galaxy light profiles can be found in Erwin, Graham & Caon (2004) and Trujillo et al. (2004).

Table 1. SMBH galaxy sample. Column (1): galaxy names; eight galaxies marked with an asterisk (*) have been excluded from the final analysis due to the large disagreement on their Sérsic index measurements, according to the criteria mentioned in Section 2.4. Column (2): morphological type as listed by Graham & Scott (2013), primarily from NED. Column (3): absolute total *B*-band magnitudes, from the RC3 catalogue using the galaxy distances published in Graham & Scott (2013). Column (4): black hole masses from Graham & Scott (2013). Column (5): presence of a partially depleted core as listed by Graham & Scott (2013) and such that the question mark is used when the classification has come from the velocity dispersion criteria mentioned in Section 3. Columns (6–9): galaxy decomposition performed by the four works described in Section 2.2; B = Sérsic profile, D = disc, g = Gaussian, m = central mask, b = bar, p = PSF. Columns (10–13): measured Sérsic index values.

Galaxy	Type	$M_{\rm B_T}$	$M_{\rm BH}$	Core	Decomposition				n			
					GD07[a]	V12[b]	S11[c]	B12[d]	GD07[a]	V12[b]	S11[c]	B12[d]
		(mag)	(10^8 M$_\odot$)									
(1)	(2)	(3)	(4)	(5)	(6)	(7)	(8)	(9)	(10)	(11)	(12)	(13)
Abell 1836-BCG	E1	−21.43	39^{+4}_{-5}	y?				BD				2.73
Circinus	Sb	−15.14	$0.011^{+0.002}_{-0.002}$	n?			BD				2.0	
IC 1459	E	−21.30	24^{+10}_{-10}	y			Bg				6.0	
IC 2560	SBb	−20.52	$0.044^{+0.044}_{-0.022}$	n?			BDg				2.0	
MESSIER 32	S0?	−15.46	$0.024^{+0.005}_{-0.005}$	n	BD	BDm	BD		1.51	2.1	4.0	
MESSIER 59	E	−20.68	$3.9^{+0.4}_{-0.4}$	n		Bm	B			5.7	5.0	
MESSIER 60	E1	−21.26	47^{+10}_{-10}	y	B	Bm	BD	BD	6.04	3.6	3.0	1.63
MESSIER 64	Sab	−19.96	$0.016^{+0.004}_{-0.004}$	n?				BD				1.49
MESSIER 77	SBb	−21.30	$0.084^{+0.003}_{-0.003}$	n		BDbm	BDg	BD		0.8	1.0	1.27
MESSIER 81	Sab	−20.01	$0.74^{+0.21}_{-0.11}$	n	BD		BDg	BD	3.26		3.0	2.57
MESSIER 84	E1	−21.17	$9^{+0.9}_{-0.8}$	y	B	Bm	Bg	B	5.60	3.5	7.0	4.10
MESSIER 87*	E0	−21.38	$58^{+3.5}_{-3.5}$	y?	B	Bm	Bg		6.86	2.4	4.0	
MESSIER 89	E	−20.14	$4.7^{+0.5}_{-0.5}$	y		B	BDg	B		3.6	4.0	4.30
MESSIER 96	SBab	−19.91	$0.073^{+0.015}_{-0.015}$	n			BDb				1.0	
MESSIER 104	Sa	−20.91	$6.4^{+0.4}_{-0.4}$	y			BDbg				1.5	
MESSIER 105	E1	−19.82	4^{+1}_{-1}	y	B		B		4.29		5.0	
MESSIER 106	SBbc	−20.19	$0.39^{+0.01}_{-0.01}$	n	BD	BDp	BDg		2.04	3.5	2.0	
Milky Way	SBbc		$0.043^{+0.004}_{-0.004}$	n	BD				1.32			
NGC 0524	S0	−20.54	$8.3^{+2.7}_{-1.3}$	y			BD				3.0	
NGC 0821	E	−20.18	$0.39^{+0.26}_{-0.09}$	n	B		B	B	4.00		7.0	7.70
NGC 1023	SB0	−19.88	$0.42^{+0.04}_{-0.04}$	n	BD		BDb		2.01		3.0	
NGC 1300	SBbc	−20.47	$0.73^{+0.69}_{-0.35}$	n			BD				3.0	
NGC 1316	SB0	−21.93	$1.5^{+0.75}_{-0.8}$	y?			BDg				5.0	
NGC 1399	E	−20.89	$4.7^{+0.6}_{-0.6}$	y	B				16.8			
NGC 2549	SB0	−18.26	$0.14^{+0.02}_{-0.13}$	n			BD				7.0	
NGC 2778	SB0	−18.39	$0.15^{+0.09}_{-0.1}$	n	BD	BD	BD		1.60	2.7	2.5	
NGC 2787*	SB0	−17.50	$0.4^{+0.04}_{-0.05}$	n	BD		BDbg		1.97		3.0	
NGC 2960	Sa?	−21.25	$0.12^{+0.005}_{-0.005}$	n?		BD				4.0		
NGC 2974	E	−19.73	$1.7^{+0.2}_{-0.2}$	n			Bg				3.0	
NGC 3079	SBc	−20.04	$0.024^{+0.024}_{-0.012}$	n?			BDbg				2.0	
NGC 3115*	S0	−20.00	$8.8^{+10}_{-2.7}$	n	BD		BD		13.0		3.0	
NGC 3227	SBa	−20.44	$0.14^{+0.1}_{-0.06}$	n			BD				4.0	
NGC 3245	S0	−19.84	$2^{+0.5}_{-0.5}$	n	BD	BD	BD	BD	4.31	2.6	2.5	1.60
NGC 3377	E5	−18.95	$0.77^{+0.04}_{-0.06}$	n	B		B	B	3.04		6.0	3.47
NGC 3384	SB0	−19.42	$0.17^{+0.01}_{-0.02}$	n	BD		BDb	BD	1.72		2.5	2.33
NGC 3414	S0	−19.99	$2.4^{+0.3}_{-0.3}$	n			BDb				5.0	
NGC 3489	SB0	−19.22	$0.058^{+0.008}_{-0.008}$	n			BD				1.5	
NGC 3585	S0	−20.57	$3.1^{+1.4}_{-0.6}$	n			BD				2.5	
NGC 3607	S0	−20.91	$1.3^{+0.5}_{-0.5}$	n			Bg	B			5.0	4.70
NGC 3608*	E2	−20.04	$2^{+1.1}_{-0.6}$	y			B	B			6.0	9.03
NGC 3998*	S0	−19.07	$8.1^{+2}_{-1.9}$	y?			BDg	BD			1.5	2.29
NGC 4026	S0	−18.93	$1.8^{+0.6}_{-0.3}$	n			BD				3.5	
NGC 4151	SBab	−20.01	$0.65^{+0.07}_{-0.07}$	n			BDg				3.5	
NGC 4261	E2	−21.03	5^{+1}_{-1}	y	B	Bm	BDg	B	7.30	3.5	4.0	4.31

Table 1 – *continued*

Galaxy	Type	M_{B_T}	M_{BH}	Core	Decomposition				*n*			
					GD07[a]	V12[b]	S11[c]	B12[d]	GD07[a]	V12[b]	S11[c]	B12[d]
		(mag)	$(10^8 M_\odot)$									
(1)	(2)	(3)	(4)	(5)	(6)	(7)	(8)	(9)	(10)	(11)	(12)	(13)
NGC 4291	E2	−19.60	$3.3^{+0.9}_{-2.5}$	y	B				4.02			
NGC 4342*	S0	−18.40	$4.5^{+2.3}_{-1.5}$	n	BD	BD			5.11	1.9		
NGC 4459*	S0	−19.66	$0.68^{+0.13}_{-0.13}$	n		B	BD	B		3.9	2.5	7.44
NGC 4473	E5	−19.76	$1.2^{+0.4}_{-0.9}$	n	B	Bm	B	BD	2.73	4.3	7.0	2.23
NGC 4486A	E2	−18.04	$0.13^{+0.08}_{-0.08}$	n		Bm	B			2.0	2.5	
NGC 4564	S0	−18.77	$0.6^{+0.03}_{-0.09}$	n	BD	BD	BD		3.15	3.7	7.0	
NGC 4596	SB0	−19.80	$0.79^{+0.38}_{-0.33}$	n		BDb	BDb	BD		3.6	3.0	4.43
NGC 4697	E4	−20.14	$1.8^{+0.2}_{-0.1}$	n	B	B	B	B	4.00	3.8	5.0	4.96
NGC 5077	E3	−20.69	$7.4^{+4.7}_{-3}$	y			Bg				6.0	
NGC 5128	S0	−20.06	$0.45^{+0.17}_{-0.1}$	n?			BDbg				3.5	
NGC 5252	S0	−21.03	11^{+16}_{-5}	n				BD				4.82
NGC 5576	E3	−20.12	$1.6^{+0.3}_{-0.4}$	n		Bm	B	B		5.1	7.0	8.71
NGC 5813	E	−21.03	$6.8^{+0.7}_{-0.7}$	y		Bm	B			8.3	6.0	
NGC 5845	E3	−18.51	$2.6^{+0.4}_{-1.5}$	n	B	B	B	B	3.22	2.6	3.0	3.45
NGC 5846	E	−20.87	11^{+1}_{-1}	y		Bm	B			3.7	3.0	
NGC 6251*	E2	−21.46	5.9^{+2}_{-2}	y?	B		Bg		11.8		7.0	
NGC 7052	E	−20.71	$3.7^{+2.6}_{-1.5}$	y	B	BD	B		4.55	1.8	5.0	
NGC 7582	SBab	−20.34	$0.55^{+0.26}_{-0.19}$	n			BDg				4.0	

[a] Graham & Driver (2007b). [b] Vika et al. (2012). [c] Sani et al. (2011). [d] Beifiori et al. (2012).

Deep Sky Survey Large Area Survey (UKIDSS-LAS); Lawrence et al. (2007)] of a sample of 25 galaxies. V12 fit the light distribution using a Sérsic function for the elliptical galaxies, the bulges and the bars of lenticular/spiral galaxies and an exponential function for the disc components. In the case of core-Sérsic galaxies with partially depleted cores, they implemented a mask for the inner region. Bright nuclei were additionally modelled as point sources using the point spread function (PSF). A relation between SMBH mass and the Sérsic index was not found by V12. They noticed that the Sérsic index can vary significantly from study to study and they suggested that such mismatch may be due to the different weighting of pixels during the fit that each study used and/or to a wavelength bias. The signal-to-noise-weighted fitting routines, such as GALFIT, can be highly sensitive to central dust obscuration, unaccounted for central excesses and deficits of light relative to the fitted model, and especially errors in the adopted PSF.

(iii) From their GALFIT3-derived 2D bulge-disc decompositions of *Spitzer*/IRAC 3.6 μm images of 57 galaxies, Sani et al. (2011, hereafter S11) investigated the scaling relations between SMBH mass and several other parameters of the host spheroids. The image decomposition was performed with a Sérsic model for the elliptical galaxies and with a Sérsic model plus an exponential model for the lenticular and spiral galaxies. A Gaussian component and a nuclear point source were added in the presence of a bar or an AGN, respectively. In an attempt to restrict the degeneracy between the effective radius and the Sérsic index, following Hunt, Pierini & Giovanardi (2004), S11 performed 2D fitting by fixing the Sérsic index to a set of constant values in the range between $n = 1$ and $n = 7$. They found tight correlations between the SMBH mass and the bulge luminosity and dynamical mass. However, the relation between the SMBH mass and the effective radius had a high intrinsic dispersion and no correlation with the Sérsic index was found.

(iv) Beifiori et al. (2012, hereafter B12) analysed SDSS *i*-band images and extracted photometric and structural parameters for a sample of 57 galaxies, for which 19 had an accurate M_{BH} measurement and the remaining 38 had only an upper limit which are not used here. They performed 2D decompositions with GASP2D (Méndez-Abreu et al. 2008), using a Sérsic profile to model the elliptical galaxies and a combination of a Sérsic plus an exponential model for the disc galaxies. Galaxies affected by poor decomposition due to either a central bar, a Freeman Type II disc profile (Freeman 1970), or just inadequately represented by the single or double component modelling were eliminated from their initial sample. Among their correlations involving the SMBH mass and the parameters of the host galaxy, the tightest was with the stellar velocity dispersion. Little or no correlation was found with the Sérsic index (see their fig. 7).

Table 1 reports the Sérsic index measurements from the above four works, along with the type of photometric decomposition performed. It comprises 62 galaxies. Each galaxy can have up to four Sérsic index estimates. 35 galaxies have multiple measurements of their Sérsic index. In the next two Sections we discuss how we compare and combine them.

2.3 Comparing Sérsic indices

There are three main points that distinguish each study: the first is the wavelength of the image.

The spatial distribution of the surface brightness of a galaxy, and hence its light profile, is a function of the observational bandpass. This means that the structural parameters, in general, may vary with wavelength due to stellar population gradients or dust obscuration. The central light concentration of a galaxy, described by the Sérsic index, is indeed a slight function of wavelength. Using reprocessed

Sloan Digital Sky Survey Data Release Seven (SDSS DR7, Abazajian et al. 2009) and UKIDSS-LAS (Lawrence et al. 2007) imaging data available from the GAMA data base, Kelvin et al. (2012) performed 2D model fits with GALFIT to ∼170 000 galaxies in the *ugrizYJHK* bandpasses, using primarily a pure Sérsic profile, to quantify how photometric and structural parameters of a galaxy vary with wavelength. Their fig. 21 shows the mean Sérsic index as a function of the rest-frame wavelength for two subsamples: the disc-dominated and the spheroid-dominated systems. Kelvin et al. (2012) find that the spheroid-dominated population is characterized by mean Sérsic indices that remain relatively stable at all wavelengths, with n increasing by 30 per cent from g to K.

The second point is the model-fitting method: one-dimensional and two-dimensional photometric decomposition techniques, if performed on the same galaxy, can produce different values of the Sérsic index due to ellipticity gradients which the 2D models cannot accommodate. The parameters of the Sérsic model can vary if derived along the major or the minor axis, as first noted by Caon et al. (1993). Ferrari et al. (2004) quantified such discrepancy in terms of ellipticity gradients, i.e. the isophote eccentricity that varies with radius. The histogram in Fig. 1 has been created using data from Caon et al. (1993) and shows the distribution of the ratio between the 'equivalent' Sérsic index $n_{\rm eq}$ and that measured along the major axis, $n_{\rm maj}$. The 'equivalent' axis is the geometric mean, $\sqrt{ab}$, of the major and the minor axis of the isophotal ellipses. The mean (and the standard deviation) of the whole sample is $\langle n_{\rm eq}/n_{\rm maj} \rangle = 1.10 \pm 0.27$. This tells us that the equivalent Sérsic index is on average 10 per cent higher than the major axis Sérsic index. From Fig. 1, their relative difference will be less than 40 per cent in 95 per cent of the time.

The third issue pertains to the weighting scheme used for the fits. The arrival of photons, which build up a galaxy image, is a Poissonian process (noise $\propto \sqrt{\rm signal}$), which therefore advocates the need for a signal-to-noise-weighted fitting scheme. However, the presence of AGNs, nuclear star clusters, nuclear stellar discs, dust, partially depleted cores and an uncertain PSF make such a weighting prone to error unless all of these factors are taken into account.

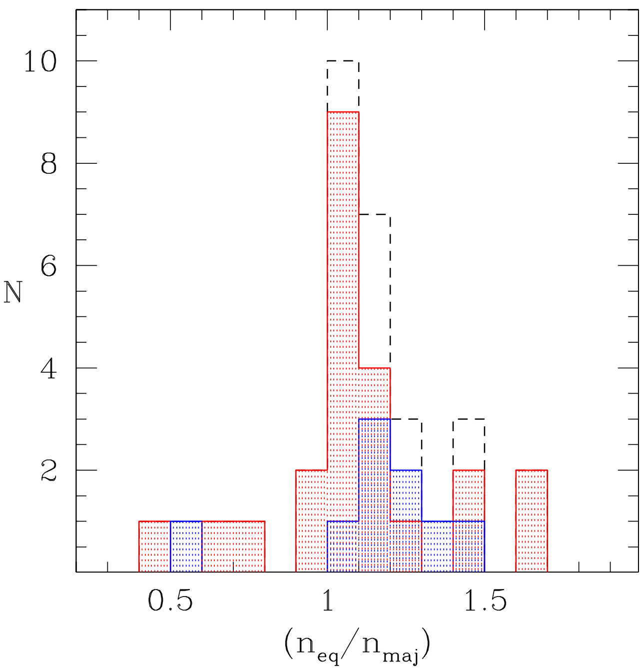

Figure 1. Distribution of the ratio between the "equivalent" Sérsic index $n_{\rm eq}$ and that measured along the major-axis $n_{\rm maj}$. Data are taken from Caon et al. (1993). The red histogram is for elliptical galaxies, while the blue is for lenticular galaxies and the black dashed line represents the whole sample.

Hence, what do we expect from our heterogeneous collection of data? First, the wavelength bias should produce a systematic effect in the Sérsic index measurements, i.e. we expect the measurements from GD07 (R band) and B12 (i band) to be slightly smaller than those from V12 (K band) and S11 (3.6 µm). Secondly, because the Sérsic index derived from a two-dimensional analysis can be approximated to the one-dimensional $n_{\rm eq}$, one may expect the Sérsic index derived from one-dimensional decomposition along the major axis, as performed by GD07, to be slightly smaller than the Sérsic index derived from the two-dimensional modelling in V12, S11 and B12. However, when we compare different measurements of the Sérsic index (belonging to the same galaxy), we do not observe the previous systematic effects; moreover, for a non-negligible number of galaxies we find that multiple measurements have a relative difference[3] greater than 50 per cent.

Many factors, if not properly taken into account, can affect the model fitting of the light distribution of a galaxy and hence the derivation of its structural parameters. These factors can include: additional nuclear components, the presence of a bar, a partially depleted core in high-resolution images, a bad sky subtraction, etc. Moreover, different choices of structural components for the same galaxy will produce contrasting Sérsic indices. Table 2 reports a few examples of discrepant measurements. For the first five galaxies, each study used the same type of decomposition (Sérsic or Sérsic+exponential). For the last three galaxies, each study performed a different image decomposition. M60 was modelled with a pure Sérsic profile by GD07 and V12, while S11 and B12 used an additional disc component. NGC 4459 has a bulge+disc profile according to S11, while V12 and B12 agreed in modelling the galaxy with a pure Sérsic profile. GD07 and S11 fit NGC 7052 with a pure Sérsic profile, whereas V12 chose a bulge+disc model. An exhaustive analysis of why the individual Sérsic indices differ from author to author is however beyond the scope of this work.

2.4 Combining Sérsic indices

To combine the results of these four heterogeneous works, we decided to use a method that was as simple as possible and that involved the least manipulation of the data. Our strategy consisted of looking at galaxies with multiple measurements, comparing the different Sérsic indices and excluding the most contrasting measurements before then averaging the remaining Sérsic indices.

The exclusion algorithm is the following: given a galaxy A that has been analysed by more than one study, we take each measurement $n_{\rm i}^{\rm A}$ and we look for the closest one $n_{\rm j}^{\rm A}$. If the absolute difference $|\Delta n_{\rm ij}^{\rm A}| = |n_{\rm i}^{\rm A} - n_{\rm j}^{\rm A}|$ is more than 50 per cent of the minimum among the two measurements, we exclude $n_{\rm i}^{\rm A}$. Obviously, if a galaxy has only two measurements, we exclude both of them. After applying the exclusion algorithm, we compute the average logarithmic value of the remaining measurements to give us $\langle \log (n^{\rm A}) \rangle$.

Figs 2 and 3 are helpful to visualize our approach. Fig. 3 is a 'zoom' of Fig. 2 and they both show the absolute total B-band magnitude $M_{B_{\rm T}}$ of elliptical galaxies plotted against their Sérsic

[3] Given two measurements n_1 and n_2, with $n_1 < n_2$, we define the *relative difference* as $(n_2 - n_1)/n_1$.

Table 2. Examples of outlying measurements, used to explain the crossed out data in Fig. 3. Column (1): galaxy names. Columns (2,4,6,8): literature Sérsic index measurements in ascending order; the reference is given in the superscript. Columns (3,5,7): relative differences; bold type is used for values greater than 50 per cent.

Galaxy (1)	n_1 (2)	$\frac{n_2-n_1}{n_1}$ (3)	n_2 (4)	$\frac{n_3-n_2}{n_2}$ (5)	n_3 (6)	$\frac{n_4-n_3}{n_3}$ (7)	n_4 (8)
Galaxies with same choice of decomposition							
M87	$2.4^{\rm V12}$	**0.67**	$4.0^{\rm S11}$	**0.72**	$6.86^{\rm GD07}$		
NGC 0821	$4.0^{\rm GD07}$	**0.75**	$7.0^{\rm S11}$	0.10	$7.70^{\rm B12}$		
NGC 3115	$3.0^{\rm S11}$	**3.33**	$13.0^{\rm GD07}$				
NGC 4342	$1.9^{\rm V12}$	**1.69**	$5.11^{\rm GD07}$				
NGC 4564	$3.15^{\rm GD07}$	0.17	$3.7^{\rm V12}$	**0.89**	$7.0^{\rm S11}$		
NGC 6251	$7.0^{\rm S11}$	**0.69**	$11.8^{\rm GD07}$				
Galaxies with different choices of decomposition							
M60	$1.63^{\rm B12}$	**0.84**	$3.0^{\rm S11}$	0.20	$3.6^{\rm V12}$	**0.68**	$6.04^{\rm GD07}$
NGC 4459	$2.5^{\rm S11}$	**0.56**	$3.9^{\rm V12}$	**0.91**	$7.44^{\rm B12}$		
NGC 7052	$1.8^{\rm V12}$	**1.53**	$4.55^{\rm GD07}$	0.10	$5.0^{\rm S11}$		

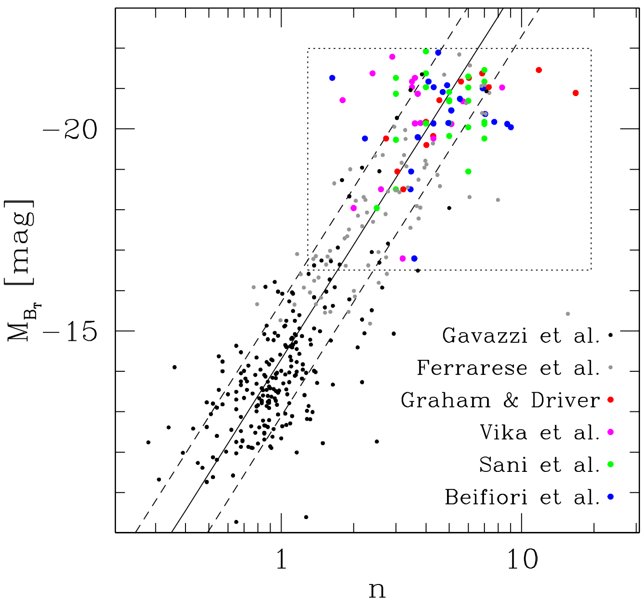

Figure 2. Absolute *B*-band magnitude versus Sérsic index of elliptical galaxies. Black points are measurements from Gavazzi et al. (2005); grey points are from Ferrarese et al. (2006); red points are from GD07; pink points are from V12; green points are from S11; blue points are from B12. The black points from Gavazzi et al. (2005) and the grey points from Ferrarese et al. (2006) have been plotted just for illustrative purposes, but they will be ignored in the following analysis because they are not from a black hole sample. Each galaxy can have more than one Sérsic measurement and hence may be represented more than once along the horizontal axis (with different colours). The black solid line shows the elliptical galaxy $M_{B_T} - n$ relation from Graham & Guzmán (2003), while the dashed lines are a rough "by eye" estimate of the scatter from their diagram. The dotted box marks the region that is shown in Fig. 3.

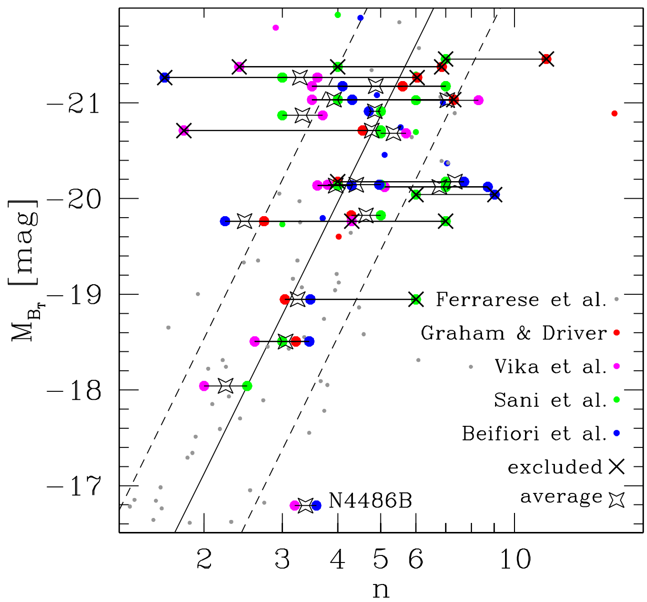

Figure 3. Absolute *B*-band magnitude versus Sérsic index of elliptical galaxies. This figure is a 'zoom' of the dotted box in Fig. 2 and it uses the same colour coding (see the previous caption). The black solid line and the dashed lines are again the $M_{B_T}-n$ relation from Graham & Guzmán (2003) and a rough 'by eye' estimate of the scatter in their diagram. The grey points are excluded from the following description. Horizontal solid lines connect different Sérsic measurements of the same galaxy. Bigger dots refer to galaxies with multiple measurements, while smaller dots show galaxies with only one measurement. The black crosses mark the excluded measurements, according to the algorithm described in Section 2.4 and illustrated in Table 2. Big empty stars indicate the average Sérsic index $\langle \log(n) \rangle$ derived from the 'good' (not excluded) Sérsic measurements.

index. The black solid line shows the $M_{B_T}-n$ relation from Graham & Guzmán (2003) such that $M_{B_T} = -9.4\log(n) - 14.3$, while the dashed lines are a rough 'by eye' estimate of its scatter.

The horizontal solid lines in Fig. 3 connect the different Sérsic index measurements of the same galaxy. If a galaxy's Sérsic index has been measured by more than one study, it is represented with a bigger dot. Thus, small dots refer to galaxies that have been measured by only one study. A black cross on a dot means that we intend to exclude that particular measurement because it is in strong disagreement (>50 per cent) with the other points according to our exclusion algorithm. The average $\langle \log(n^{\rm A}) \rangle$ of the logarithmic values of the remaining measurements is denoted by an empty star.

We apply the same procedure to the bulges of the lenticular and spiral galaxies, which are not shown in the $M_{B_T}-n$ plots (Figs 2 and 3), but are included in the following analysis. Our final sample consists of 54 galaxies with directly measured SMBH mass and at least one measurement of the Sérsic index; among these, 27 galaxies

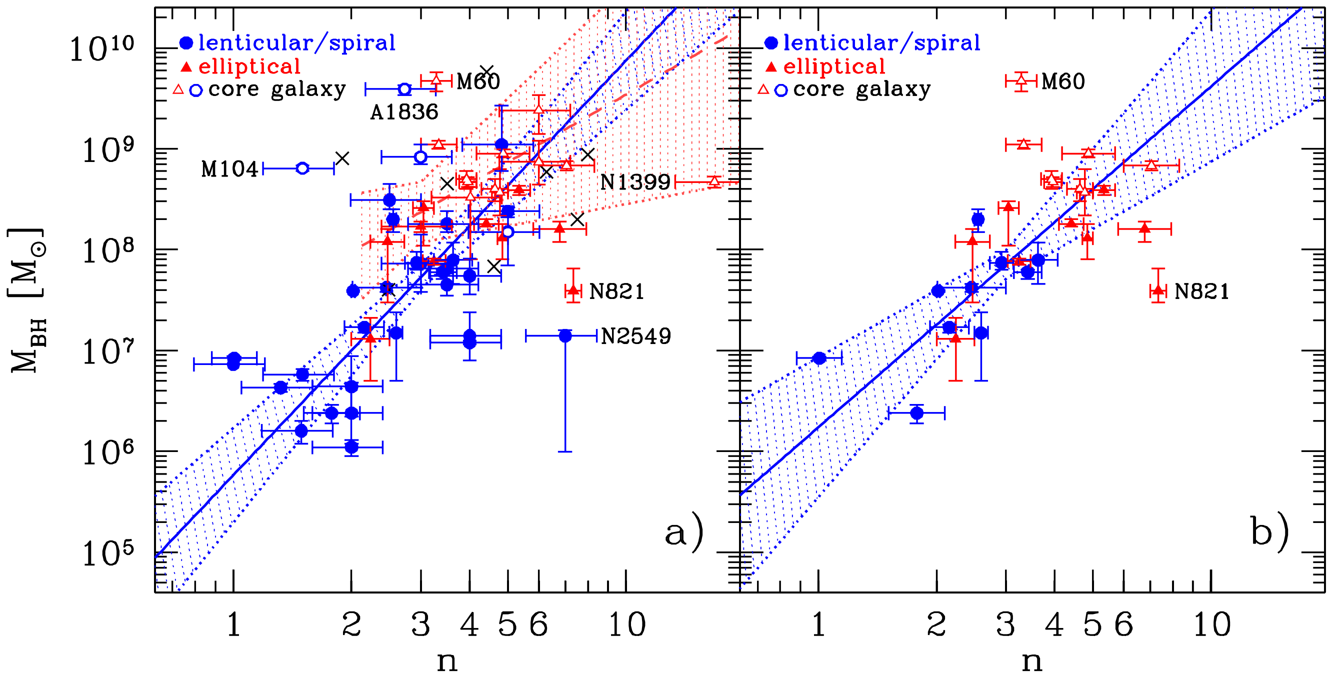

Figure 4. Black hole mass versus Sérsic index. Fig. 4(a): all galaxies with at least one measurement from GD07, V12, S11 and B12; if a galaxy has been measured by more than one study, we plot the average value of its Sérsic index as obtained in Section 2.4. The black crosses are used to show the location of the eight galaxies excluded from the initial sample of 62, due to widely varying Sérsic indices (we plot their mean Sérsic index). Fig. 4(b): only the 27 galaxies with multiple Sérsic measurements. Open symbols are used for core-Sérsic galaxies, rather than filled symbols that denote Sérsic galaxies. The solid blue line (and the blue dotted lines) shows the symmetrical bisector regression (with errors) for the Sérsic bulges of disc galaxies. The dashed red line (and the red dotted lines) shows the symmetrical bisector regression (with errors) for core-Sérsic elliptical galaxies (not shown in Fig. 4(b) due to the low number statistics). The labelled galaxies designate outliers that were excluded from the regressions.

have indices measured by more than one study. The eight galaxies excluded from the initial sample of 62 objects, due to widely varying Sérsic indices, are marked with a star in Table 1.

3 ANALYSIS

After taking galaxies with multiple Sérsic index measurements, rejecting the outlying values and averaging the remaining ones, according to the strategy discussed in Section 2.4, we build the $M_{\rm BH}$–n diagram. For galaxies with multiple measurements, we calculated the error on their mean Sérsic index, whereas for single-measured objects we assumed an error[4] of 20 per cent. Fig. 4(a) includes galaxies with single and averaged-multiple Sérsic indices, whereas Fig. 4(b) only shows those with an averaged-multiple measurement and is thus more reliable.

Despite the higher level of scatter in Fig. 4(a), both diagrams display an appreciable correlation between the SMBH mass and the spheroid light concentration. That is, after excluding the discrepant Sérsic indices according to the process in Section 2.4, presumably from poor fits, we recover a clear trend between black hole mass and Sérsic index. We have visually identified six[5] outliers in Fig. 4(a) and two[6] outliers in Fig. 4(b); these objects are labelled in both diagrams and were excluded from the following regression analysis. The Spearman's correlation coefficients r_s and the likelihood of the correlation occurring by chance P are given in Table 3. In both panels, we have performed a symmetrical linear bisector regression using the BCES routine from Akritas & Bershady (1996), which was checked using the Bayesian linear regression code LINMIX_ERR (Kelly 2007). However, we have not lumped all the galaxy data together, as there is good reason not to do this.

Table 3. Spearman's correlation coefficients $r_s(N-2)$ and likelihood of the correlation occurring by chance P. $N-2$ are the degrees of freedom.

Fig. 4(a) excluding outliers	$r_s(46) = 0.72$	$P < 0.1$ per cent
Fig. 4(a) including outliers	$r_s(52) = 0.53$	$P < 0.1$ per cent
Fig. 4(b) excluding outliers	$r_s(23) = 0.76$	$P < 0.1$ per cent
Fig. 4(b) including outliers	$r_s(25) = 0.60$	$P < 1$ per cent

Among our galaxy sample with direct $M_{\rm BH}$ measurements, Graham & Scott (2013) identified 'core-Sérsic' galaxies that display a central deficit of light relative to the inward extrapolation of their outer Sérsic light profile, and 'Sérsic' galaxies that do not (Graham & Guzmán 2003; Graham et al. 2003; Trujillo et al. 2004). 'Core-Sérsic' galaxies are thought to have formed from dry merger events, whereas 'Sérsic' galaxies are the result of gaseous processes. Their classification (Column 5 of Table 1) has primarily come from the inspection of high-resolution images. When no core designation was available or possible from the literature, Graham & Scott (2013) used a criteria based on the velocity dispersion σ, such that galaxies with $\sigma > 270$ km s^{-1} are considered likely to possess a partially depleted core, while galaxies with $\sigma < 165$ km s^{-1} are

[4] The error of single-measured objects was estimated as follows. Using the 35 galaxies with multiple measurements of their Sérsic indices, we first computed the average $\langle \log(n) \rangle$ of each galaxy without applying the exclusion algorithm (see Section 2.4) and its error $\sigma_{\langle \log(n) \rangle}$; we then calculated the median value of the errors $\langle \sigma_{\langle \log(n) \rangle} \rangle = 0.08$ (20 per cent).

[5] Abell 1836-BCG, M60, M104, NGC 1399, NGC 821, NGC 2549.

[6] M60, NGC 821.

Table 4. Observed $M_{\rm BH}-n$ scaling relations. $M_{\rm BH}$ = black hole mass, n = Sérsic index. A symmetrical bisector regression (BCES routine from Akritas & Bershady 1996) was used. The quantity n is normalized to the round median value of the distribution of the Sérsic indices for the SMBH galaxy sample ($\langle n \rangle = 3$). The total rms scatter in the $\log(M_{\rm BH})$ direction is denoted by Δ.

Number	Type	α	β	Δ dex
	Fig. 4(a) $\log(M_{\rm BH}/{\rm M}_\odot) = \alpha + \beta \log(n/3)$			
9	Sérsic elliptical galaxies	–	–	–
27	Sérsic bulges	7.73 ± 0.12	4.11 ± 0.72	0.62
10	Core-Sérsic elliptical galaxies	8.37 ± 0.30	2.23 ± 1.50	0.27
2	Core-Sérsic bulges	–	–	–
	Fig. 4(b) $\log(M_{\rm BH}/{\rm M}_\odot) = \alpha + \beta \log(n/3)$			
8	Sérsic elliptical galaxies	–	–	–
10	Sérsic bulges	7.85 ± 0.14	3.38 ± 1.16	0.44
7	Core-Sérsic elliptical galaxies	–	–	–
0	Core-Sérsic bulges	–	–	–

not. For reasons discussed in Section 4, we divided our sample into four subsamples:

(i) the Sérsic bulges of disc galaxies;
(ii) Sérsic elliptical galaxies;
(iii) the core-Sérsic bulges of disc galaxies;
(iv) core-Sérsic elliptical galaxies.

We expect a different $M_{\rm BH}-n$ relation for each of the previous subsamples, and hence we elect not to perform a single linear regression to all the data shown in Figs 4(a) and 4(b). Our symmetrical regressions have been performed for the Sérsic bulges of disc galaxies in Figs 4(a) and 4(b) and for core-Sérsic elliptical galaxies in Fig. 4(a). Due to small numbers, the statistics were not able to provide reliable regressions for core-Sérsic elliptical galaxies in Fig. 4(b), nor for Sérsic elliptical galaxies and core-Sérsic bulges in either Figs 4(a) and 4(b). Table 4 contains the results from the symmetrical regressions. All of the outliers reside more than 3σ from the linear regressions.

4 PREDICTIONS AND DISCUSSION

The $M_{\rm BH}-n$ relation can be predicted from two other important scaling relations: the $M_{\rm BH}-L_{\rm sph}$ and the $L_{\rm sph}-n$ relations, where $L_{\rm sph}$ is the luminosity of the galaxy's spheroidal component.

Since at least Graham (2001, his fig. 14), we have known that the $L_{\rm sph}-n$ relation is different for elliptical galaxies and the bulges of disc galaxies. fig. 10 from Graham & Guzmán (2003) and fig. 11 from Graham (2013) display the $L_{\rm sph}-n$ relation for elliptical galaxies (in the B-band) and for the bulges of disc galaxies (in the $K_{\rm s}$ band), respectively. In both figures, the linear regressions had been estimated 'by eye'. We re-analysed the data from their figures and performed a symmetrical linear bisector regression analysis using the BCES routine from Akritas & Bershady (1996).

We obtained

$$M_{\rm B,sph} = (-18.25 \pm 0.18) + (-9.01 \pm 0.47)\log(n/3)$$

for the elliptical galaxies, and

$$M_{\rm K_s,sph} = (-23.01 \pm 0.15) + (-5.55 \pm 0.47)\log(n/3)$$

for the bulges of the disc galaxies. Here, $M_{\rm B,\,sph}$ indicates the absolute B-band magnitude of elliptical galaxies and $M_{\rm K_s,sph}$ indicates the dust-corrected, absolute $K_{\rm s}$-band magnitude of the bulges of disc galaxies.

We have used the $M_{\rm BH}-L_{\rm sph}$ relation from Graham & Scott (2013) who derived B-band and $K_{\rm s}$-band bulge magnitudes, from the total luminosity of lenticular and spiral galaxies, through a statistical correction that takes into account inclination effects and dust absorption. Following Graham (2012), Graham & Scott (2013) derived the $M_{\rm BH}-L_{\rm sph}$ relation separately for core-Sérsic and Sérsic spheroids. They observed a near-linear $M_{\rm BH}-L_{\rm sph}$ relation for the core-Sérsic spheroids, thought to be built in additive dry merger events, and a notably (2.5 times) steeper $M_{\rm BH}-L_{\rm sph}$ relation for the Sérsic spheroids considered to be products of gas-rich processes. They reported

$$\log(M_{\rm BH}) = (9.03 \pm 0.09) + (-0.54 \pm 0.12)(M_{\rm B,sph} + 21)$$

and

$$\log(M_{\rm BH}) = (9.05 \pm 0.09) + (-0.44 \pm 0.08)(M_{\rm K_s,sph} + 25)$$

for their core-Sérsic subsample, whereas

$$\log(M_{\rm BH}) = (7.37 \pm 0.15) + (-0.94 \pm 0.16)(M_{\rm B,sph} + 19)$$

and

$$\log(M_{\rm BH}) = (7.39 \pm 0.14) + (-1.09 \pm 0.22)(M_{\rm K_s,sph} + 22.5)$$

for their Sérsic galaxies.

The *bent* nature of the above $M_{\rm BH}-L_{\rm sph}$ relations and the *linear* nature of the two distinct $L_{\rm sph}-n$ relations for elliptical galaxies and bulges requires that there be two distinct *bent* $M_{\rm BH}-n$ relations for elliptical galaxies and bulges. This explains the *curved* nature of the $M_{\rm BH}-n$ relation reported by GD07. The *predicted* $M_{\rm BH}-n$ relations, derived from the above six equations, are reported in Table 5 and shown in Fig. 5.

The expected $M_{\rm BH}-n$ relations for the Sérsic bulges of disc galaxies and for core-Sérsic elliptical galaxies (Table 5) are marginally consistent at the 2σ level with the results from the linear regression analysis performed in Fig. 4 (Table 4). More quality data and a wider range of Sérsic indices would be beneficial to confirm the predicted relations.

For comparison, in Fig. 5 we plot 10 additional galaxies with $M_{\rm BH} < 10^7\,{\rm M}_\odot$ taken from the sample of Greene et al. (2008). The horizontal offset that separates the bulges of their four disc galaxies

Table 5. Predicted $M_{BH}-n$ relations.

Type	Prediction
Sérsic elliptical galaxies	$\log(M_{BH}) = (6.66 \pm 0.26) + (8.47 \pm 1.51) \log(n/3)$
Sérsic bulges	$\log(M_{BH}) = (7.95 \pm 0.24) + (6.05 \pm 1.32) \log(n/3)$
Core-Sérsic elliptical galaxies	$\log(M_{BH}) = (7.54 \pm 0.35) + (4.87 \pm 1.11) \log(n/3)$
Core-Sérsic bulges	$\log(M_{BH}) = (8.17 \pm 0.19) + (2.44 \pm 0.49) \log(n/3)$

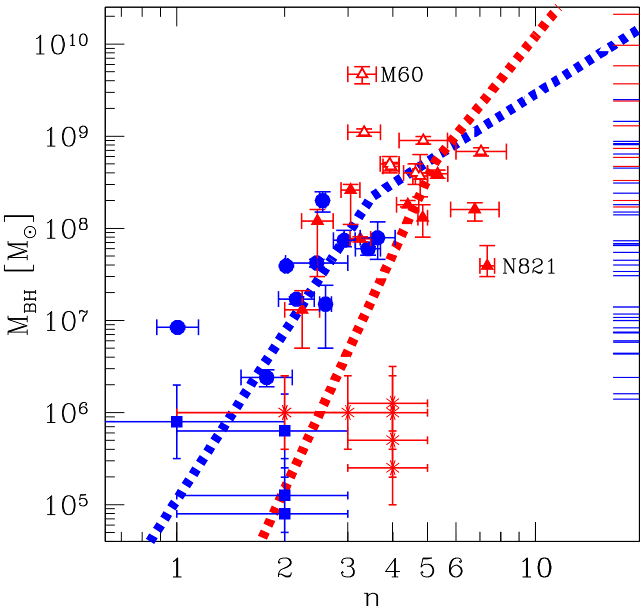

Figure 5. Same data as Fig. 4(b). For comparison, we plot four additional bulges of disc galaxies (blue squares) and six additional elliptical galaxies (red asterisks) taken from the sample of Greene, Ho & Barth (2008). The dashed lines show the *predicted* $M_{BH}-n$ relations for elliptical galaxies in red and for the bulges of disc galaxies in blue, given the *observed* $M_{BH}-L_{sph}$ and the $L_{sph}-n$ relations in the literature. The ticks on the right-hand axis indicate the black hole masses of 14 elliptical galaxies (in red) and 37 disc galaxies (in blue) that belong to the sample of Graham & Scott (2013) (and hence have a secure M_{BH} detection) but do not have multiple Sérsic index measurements.

from their six elliptical galaxies supports our predicted gap between the $M_{BH}-n$ relations for elliptical galaxies and bulges at the low-mass end of this diagram. If the *bent* $M_{BH}-L_{sph}$ relation is the same for all galaxies – irrespective of their morphology – this gap occurs because elliptical galaxies and the bulges of disc galaxies inhabit different regions of the $L_{sph}-n$ diagram (see fig. 14 in Graham 2001). That is, for a given light profile shape (i.e. Sérsic index n) the bulges of disc galaxies are brighter than elliptical galaxies. Fig. 5 allows one to predict that an order of magnitude gap is expected between the SMBH masses of Sérsic elliptical galaxies and the Sérsic bulges of disc galaxies having the same n.

In Fig. 5, we also show the black hole masses of 51 galaxies that belong to the sample of Graham & Scott (2013) but do not have multiple Sérsic index measurements. Among them, 13 are core-Sérsic elliptical galaxies, 5 are core-Sérsic bulges of disc galaxies, 1 is a Sérsic elliptical galaxy and 32 are Sérsic bulges of disc galaxies. We point out that measuring the Sérsic indices of these galaxies could add many useful points to the $M_{BH}-n$ diagram. In particular, the 13 extra core-Sérsic elliptical galaxies would allow one to better explore the $M_{BH}-n$ diagram in the high-M_{BH} end, between 10^8 and 10^{10} $M_\odot$, where most galaxies are thought to have formed from a different process, namely dry major mergers. Similarly, there are an additional 10 Sérsic bulges of disc galaxies with $M_{BH} < 10^7$ $M_\odot$ that could extend the low-M_{BH} end of the correlation.

The Sérsic index is a slight function of the observational bandpass. This dependence of galaxy structural parameters with wavelength arises due to radial gradients in the stellar population gradients and/or dust obscuration (Kelvin et al. 2012). We therefore plan to perform accurate galaxy image decompositions for all the galaxies belonging to the sample of Graham & Scott (2013) – with a directly measured SMBH mass – to explore the $M_{BH}-n$ relation and other black hole mass scaling relations in a homogeneous analysis (same observational bandpass and same light profile decomposition method).

Finally, we compare the results from this work with those from GD07, highlighting two main points. First, and similar to our sample, the galaxy sample used by GD07 was dominated (∼80 per cent) by disc galaxies in the low-mass end ($M_{BH} < 10^8$ $M_\odot$) and by elliptical galaxies (∼80 per cent) in the high-mass end ($M_{BH} > 10^8$ $M_\odot$). Secondly, GDO7 measured a Sérsic index greater than 10 for three spheroids with $M_{BH} \sim 10^9$ $M_\odot$, which are absent in Fig. 4(b). Combining the different galaxy types and fitting a single relation, it is easy to understand why a quadratic relation would be more appropriate than a single log-linear relation to describe their data. At $n = 3$ ($M_{BH} \sim 10^8$ $M_\odot$), their quadratic relation has a slope of 3.70 ± 0.46, similar to that observed for our Sérsic bulges.

5 SUMMARY AND CONCLUSIONS

The $M_{BH}-n$ relation (GD07) is important for any complete theory or model to describe the co-evolution of galaxies and SMBHs. It also provides a means to estimate black hole masses in galaxies and may prove fruitful for recent and future deep, wide-field photometric surveys of galaxies which can statistically estimate the black hole masses in a large sample of galaxies up to $z \sim 0.1$. The main motivation of this work was to re-investigate the $M_{BH}-n$ relation, given a recent spate of papers which did not detect it. We have gone beyond the simple recovery of the $M_{BH}-n$ relation, and explored potential substructures in this diagram in terms of distinct relations for Sérsic and core-Sérsic galaxies, and for bulges and elliptical galaxies.

We compiled a large collection of literature Sérsic index measurements GD07, S11, V12, B12) for a sample of 62 galaxies with directly measured SMBH masses. We compared multiple Sérsic index measurements which existed for 35 galaxies, and found relative differences greater than 50 per cent in many instances. This is more than expected from a systematic bias produced by different types of light profile modelling (1D or 2D) or different observational bandpasses. We therefore excluded the outlying Sérsic indices and averaged the remaining values. This exclusion resulted in the removal of eight galaxies. Our final sample therefore consists of 54 galaxies: among them, 27 had Sérsic indices measured only by one study and the remaining 27 have an averaged Sérsic index measurement.

Our principal conclusions are as follows.

(i) The $M_{\rm BH}-n$ diagram (Fig. 4) displays an appreciable correlation.

(ii) The results from the symmetrical linear regressions (Fig. 4) are consistent at the 2σ level with predictions (Fig. 5) obtained by combining the $M_{\rm BH}-L_{\rm sph}$ relations for core-Sérsic and Sérsic galaxies with the $L_{\rm sph}-n$ relations for elliptical galaxies and the bulges of disc galaxies.

(iii) If Sérsic bulges and Sérsic elliptical galaxies follow the same $M_{\rm BH}-L_{\rm sph}$ relation, then an order of magnitude gap is expected between the SMBH masses of Sérsic elliptical galaxies and the Sérsic bulges of disc galaxies having the same n.

A wider range of Sérsic indices would be beneficial to put tighter constraints on the observed slopes of the correlations. The catalogue of 80 directly measured SMBH masses compiled by Graham & Scott (2013) allows one to explore the $M_{\rm BH}-n$ diagram in the low- and high-mass end. We recognize the need for a well-calibrated $M_{\rm BH}-n$ relation and plan to perform accurate galaxy light profile decompositions to refine the black hole mass scaling relations.

ACKNOWLEDGEMENTS

GS thanks Dr Nicholas Scott for useful discussions. This research was supported by Australian Research Council funding through grants DP110103509 and FT110100263. AM, LKH, ES acknowledge support from grants PRIN-MIUR 2010-2011 'The dark Universe and the cosmic evolution of baryons: from current surveys to Euclid' and PRIN-INAF 2011 'Black hole growth and AGN feedback through the cosmic time'. This research has made use of the GOLDMine data base (Gavazzi et al. 2003) and the NASA/IPAC Extragalactic Database (NED) which is operated by the Jet Propulsion Laboratory, California Institute of Technology, under contract with the National Aeronautics and Space Administration.

REFERENCES

Abazajian K. N. et al., 2009, ApJS, 182, 543
Akritas M. G., Bershady M. A., 1996, ApJ, 470, 706
Allen P. D., Driver S. P., Graham A. W., Cameron E., Liske J., de Propris R., 2006, MNRAS, 371, 2
Andredakis Y. C., Peletier R. F., Balcells M., 1995, MNRAS, 275, 874
Beifiori A., Courteau S., Corsini E. M., Zhu Y., 2012, MNRAS, 419, 2497 (B12)
Berrier J. C. et al., 2013, ApJ, 769, 2
Caon N., Capaccioli M., D'Onofrio M., 1993, MNRAS, 265, 1013
Davis B. L., Berrier J. C., Shields D. W., Kennefick J., Kennefick D., Seigar M. S., Lacy C. H. S., Puerari I., 2013, ApJS, 199, 33
de Vaucouleurs G., de Vaucouleurs A., Corwin H. G., Jr, Buta R. J., Paturel G., Fouqué P., 1991, Third Reference Catalogue of Bright Galaxies. Springer, New York (RC3)
Driver S. P. et al., 2011, MNRAS, 413, 971
Erwin P., Graham A. W., Caon N., 2004, Coevolution of Black Holes and Galaxies, Cambridge Univ. Press, Cambridge
Ferrarese L., Merritt D., 2000, ApJ, 539, L9
Ferrarese L. et al., 2006, ApJS, 164, 334
Ferrari F., Dottori H., Caon N., Nobrega A., Pavani D. B., 2004, MNRAS, 347, 824
Freeman K. C., 1970, ApJ, 160, 811
Gadotti D. A., 2008, MNRAS, 384, 420
Gavazzi G., Boselli A., Donati A., Franzetti P., Scodeggio M., 2003, A&A, 400, 451
Gavazzi G., Donati A., Cucciati O., Sabatini S., Boselli A., Davies J., Zibetti S, 2005, A&A, 430, 411
Gebhardt K. et al., 2000, ApJ, 539, L13
Graham A. W., 2013, in Oswalt T. D., Keel W. C., eds, Planets, Stars and Stellar Systems, Volume 6. Springer, Berlin, p. 91
Graham A. W., 2001, AJ, 121, 820
Graham A. W., 2008, ApJ, 680, 143
Graham A. W., 2012, ApJ, 746, 113
Graham A. W., Driver S. P., 2005, PASA, 22, 118
Graham A. W., Driver S. P., 2007a, MNRAS, 380, L15
Graham A. W., Driver S. P., 2007b, ApJ, 655, 77 (GD07)
Graham A. W., Guzmán R., 2003, AJ, 125, 2936
Graham A. W., Scott N., 2013, ApJ, 764, 151
Graham A. W., Erwin P., Caon N., Trujillo I., 2001, ApJ, 563, L11
Graham A. W., Erwin P., Trujillo I., Asensio Ramos A., 2003, AJ, 125, 2951
Graham A. W., Driver S. P., Allen P. D., Liske J., 2007, MNRAS, 378, 198
Graham A. W., Onken C. A., Athanassoula E., Combes F., 2011, MNRAS, 412, 2211
Greene J. E., Ho L. C., Barth A. J., 2008, ApJ, 688, 159
Häring N., Rix H.-W., 2004, ApJ, 604, L89
Hunt L. K., Pierini D., Giovanardi C., 2004, A&A, 414, 905
Jerjen H., Binggeli B., Freeman K. C., 2000, AJ, 119, 593
Kahaner D., Moler C., Nash S., 1989, Numerical Methods and Software. Englewood Cliffs: Prentice Hall
Kelly B. C., 2007, ApJ, 665, 1489
Kelvin L. S. et al., 2012, MNRAS, 421, 1007
Kormendy J., Richstone D., 1995, ARA&A, 33, 581
Laor A., 2001, ApJ, 553, 677
Lauer T. R., Tremaine S., Richstone D., Faber S. M., 2007, ApJ, 670, 249
Lawrence A. et al., 2007, MNRAS, 379, 1599
Magorrian J. et al., 1998, AJ, 115, 2285
Marconi A., Hunt L. K., 2003, ApJ, 589, L21
McLure R. J., Dunlop J. S., 2002, MNRAS, 331, 795
Méndez-Abreu J., Aguerri J. A. L., Corsini E. M., Simonneau E., 2008, A&A, 478, 353
Pastrav B. A., Popescu C. C., Tuffs R. J., Sansom A. E., 2013, A&A, 553, A80
Peng C. Y., Ho L. C., Impey C. D., Rix H.-W., 2002, AJ, 124, 266
Peng C. Y., Ho L. C., Impey C. D., Rix H.-W., 2010, AJ, 139, 2097
Sani E., Marconi A., Hunt L. K., Risaliti G., 2011, MNRAS, 413, 1479 (S11)
Scott N., Graham A. W., Schombert J., 2013, ApJ, 768, 76
Sérsic J.-L., 1963, Boletin de la Asociacion Argentina de Astronomia La Plata Argentina, 6, 41
Sérsic J.-L., 1968, Atlas de Galaxias Australes. Observatorio Astronomico. Cordoba
Simard L. et al., 2002, ApJS, 142, 1
Simard L., Mendel J. T., Patton D. R., Ellison S. L., McConnachie A. W., 2011, ApJS, 196, 11
Trujillo I., Erwin P., Asensio Ramos A., Graham A. W., 2004, AJ, 127, 1917
Vika M., Driver S. P., Cameron E., Kelvin L., Robotham A., 2012, MNRAS, 419, 2264 (V12)
York D. G. et al., 2000, AJ, 120, 1579
Young C. K., Currie M. J., 1994, MNRAS, 268, L11

APPENDIX A

Section 2.4 illustrates the method we used to combine multiple Sérsic index measurements of the same galaxy. These came from four different studies among which only one (GD07) reported a strong $M_{\rm BH}-n$ relation.

To check the consistency and the robustness of our results, here we repeat the analysis excluding all the GD07 measurements. Fig. A1(a), which can be compared to Fig. 4(a), still displays a correlation, although it is more noisy at the high-mass end

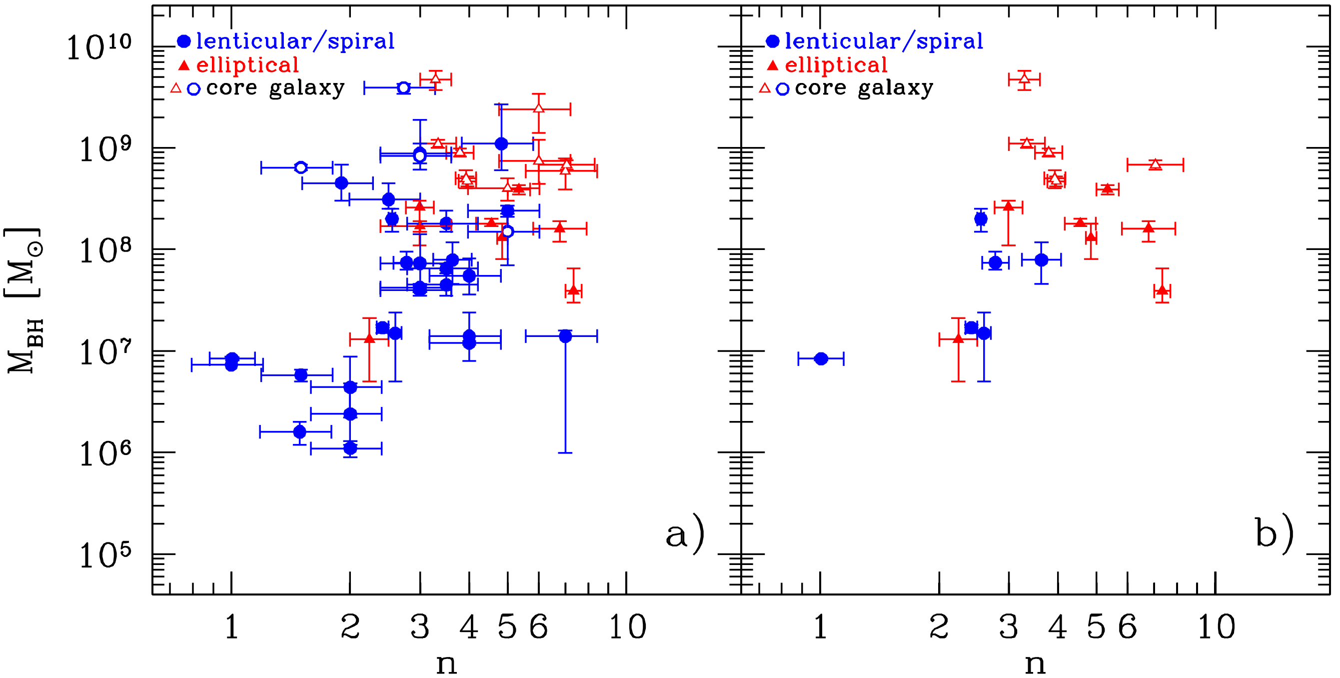

Figure A1. Same as Fig. 4 but excluding all the GD07 measurements.

(Spearman's correlation coefficient $r_s(47) = 0.38$, likelihood of the correlation occurring by chance $P < 1$ per cent). Hence, we conclude that the inclusion of the GD07 data did not force the recovery of the M_{BH}–n relation(s). However, the two galaxies previously identified as outliers in Fig. 4(b) reduce the strength of the correlationvsp in Fig. A1(b) to a likelihood of the correlation occurring by chance to $P < 5$ per cent.

This paper has been typeset from a TEX/LATEX file prepared by the author.